



## ***NONLINEAR ANALYSIS OF STEEL FIBER REINFORCED CONCRETE DEEP BEAMS BY ANSYS***

***Dr. Hayder Hussein H. Kamonna***

*University of Kufa\ College of Engineering / Civil Department*

*(Received:11/4/2010 ;Accepted :30/12/2010 )*

### **Abstract:**

*This paper considers the practical application of nonlinear models in the analysis of Steel Fiber Reinforced Concrete Deep Beams. The results of some analyses performed using the reinforced concrete model of the general purpose finite element code ANSYS are presented and discussed. Steel fiber was represented using two approaches. In the first approaches its effect in enhancement the mechanical properties of concrete is introduced. This was done by increasing the initial modulus of elasticity, compressive strength, tensile strength, ductility etc. through empirical formulas found in literatures. While the second approach was done by assuming steel fiber as smeared reinforced layers embedded in solid 65 elements. Good agreement with the experimental test was obtained by ANSYS solution. Numerical analysis showed that closed solutions were obtained with different representations of steel fiber in different orientations and number of layers. This is because that the smeared layers were assumed in each element of the structure which gave a uniform distribution for the steel fiber in deep beam. It was found that the second approaches gave better agreement with the experimental test than the first one. Assuming of steel fiber oriented in two directions with equal ratio may consider the closer one for representation of steel fiber in two dimensional structural members.*

**Key words: Deep Beam, Steel Fiber, Nonlinear Analysis, Finite Element Analysis.**

## التحليل اللاخطي للعتبات الخرسانية العميقة والمعززة بألياف حديدية باستخدام برنامج ANSYS

### الخلاصة:

هذا البحث يتضمن استخدام التحليل اللاخطي لتحليل العتبات الخرسانية والمعززة بألياف حديدية. إذ تم مناقشة بعض النتائج والتي تم الحصول عليها بنمذجة الخرسانة المسلحة باستخدام البرنامج المعروف (ANSYS) استخدم أسلوبان في هذا البحث لتمثيل الألياف الحديدية. الأسلوب الأول اعتمد تأثير الألياف الحديدية في تحسين الخواص الميكانيكية للخرسانة وباستخدام المعادلات الوضعية الموجودة في بعض المصادر. أما الأسلوب الثاني فيعتمد على تمثيل الألياف الحديدية بشكل طبقة تسليح منتشرة في العنصر solid65. لوحظ توافق جيد بين نتائج الفحص العملي و نتائج التحليل باستخدام البرنامج ANSYS. كما لوحظ إن النتائج التي تم الحصول عليها بفرض إن الألياف الحديدية هي طبقة تسليح منتشرة في العنصر solid65 كانت مقاربة جداً عند فرض إن طبقات التسليح المنتشرة تكون على شكل طبقة واحدة أو طبقتين أو ثلاث طبقات وبتجاهات مختلفة داخل العنصر solid65. وهذا يعزى إلى استخدام عناصر صغيرة لتمثيل العتب الخرساني مما يتيح أن تكون هذه الطبقات منتشرة بصورة منتظمة أكثر في جسم العتب الخرساني. لذا يمكن اعتبار تمثيل الألياف الحديدية بشكل طبقتين منتشرة و متساوية داخل العنصر solid65 هي الأقرب للواقع على فرض إن العتبات العميقة هي أعضاء إنشائية ثنائية البعد.

### 1. INTRODUCTION

Deep beams are recognized by relatively small values of span-to-depth ratio. As per code provisions given by American Concrete Institute (ACI 318-05) a beam shall be considered as deep beam when the ratio of effective span to overall depth ratio is less than 4.0 or regions with concentrated loads within twice the member depth from the face of the support. Reinforced concrete deep beams have very useful structural applications such as pile-caps, water tanks and tall buildings. Because of their proportion they develop mechanism of force transfer quite different from that in slender beams and their strength is likely to be controlled by shear rather than flexure provided with nominal amount of longitudinal reinforcement (Madana et al. 2007).

The main factors influencing SFRC tensile strength are these: volume and distribution of steel fibers in principal section, anchorage of fiber in concrete matrix, yield strength of fiber and strength of concrete (Remigijus and Gediminas 2007).

It has been well established that the use of discrete steel fibers of short length and small diameter as reinforcement improves the strength and deformational characteristics of cement based matrices. Most of the properties of fibrous concrete can be used to enhance the behavior of concrete members reinforced with conventional bar reinforcement (Madana et al. 2007).

In this paper, the ANSYS finite element program is used to simulate the behavior of fibrous reinforced concrete deep beams. The finite element model uses a smeared cracking approach, three-dimensional and one-dimensional elements to model fibrous reinforced concrete deep

beams. This model can help to confirm the theoretical calculations as well as to provide a valuable supplement to the laboratory investigations of behavior.

Many experts and scholars have studied the SRC deep beam and SFRC beam for a long time. However, the research on the SFRC deep beam is still less, and also it's difficult to simulate SFRC structure by ANSYS reasonably. **For instance, how to consider the bond stress-slip relationship and the interaction between steel bar and concrete and so on.** Furthermore, the related research reports are few. The mechanical properties of the SFRC deep beams were discussed through the nonlinear finite element method. Finally, the simulation results were compared with the test results to verify its credibility (Lihua et al. 2008).

In this work, two approaches were assumed to represent steel fibers in reinforced concrete. The first approach depends on the enhancements the mechanical properties of concrete. While in the second one, the steel fibers were assumed as smeared reinforcement layers embedded in solid 65 elements. In this approach the smeared layers were assumed in one, two and three directions. In case of one direction, it was assumed in either x-, y- or z- direction of the local coordinate system of solid 65 element. As in two direction case it was assumed in xy, xz and yz direction of the local coordinate system of solid 65 elements. But in three direction case, it was assumed that fibers to be uniformly distributed in three directions of solid 65 elements. The second case may be considered the closed one to real case.

## 2. MATERIAL CONSTITUTIVE RELATIONS

In order to obtain accurate analysis, proper material models are needed. This section presents the concrete, fibrous concrete, reinforcing steel, models that are used in this work.

### 2.1 Compressive behavior of concrete

For compression, widely accepted (Saenz's 1964) uniaxial stress-strain relationship is used in this analysis. It has the following form:

$$\sigma = \frac{E_c \varepsilon}{1 + R_3 \left(\frac{\varepsilon}{\varepsilon_o}\right) - R_2 \left(\frac{\varepsilon}{\varepsilon_o}\right)^2 + R_1 \left(\frac{\varepsilon}{\varepsilon_o}\right)^3} \quad (1)$$

where

$$\left. \begin{aligned} R_1 &= \frac{R_E (R_f - 1)}{(R_e - 1)^2} - \frac{1}{R_e} \\ R_2 &= 2R_1 - 1 \\ R_3 &= R_1 + R_E - 2 \end{aligned} \right\} \quad (2)$$

modular ratio:  $R_E = \frac{E_c}{E_o}$ , stress ratio:  $R_f = \frac{f_c}{f_c}$ , strain ratio:  $R_e = \frac{\varepsilon_f}{\varepsilon_o}$ , and secant modulus:  $E_o = \frac{f_c}{\varepsilon_o}$

Where:  $E_c$  = Initial tangent modulus,  $\sigma$  = Stress in concrete,  $\varepsilon$  = Strain in concrete,  $f_c$  = Characteristic compressive stress of concrete,  $f_f$  = Stress in the concrete at the maximum

strain,  $\epsilon_o$ =Strain in the concrete at the maximum stress,  $\epsilon_f$  = Strain in the concrete at the compressive failure (fig. 1)

The tangent modulus,  $E_t$ , corresponding to the specified strain can be found by taking derivatives of the (eq.1) with respect to strain component. This leads to:

$$E_t = \frac{d\sigma}{d\epsilon} = \frac{E_c \left[ 1 + R_2 \left( \frac{\epsilon}{\epsilon_o} \right)^2 + 2R_1 \left( \frac{\epsilon}{\epsilon_o} \right)^3 \right]^2}{\left[ 1 + R_3 \left( \frac{\epsilon}{\epsilon_o} \right) - R_2 \left( \frac{\epsilon}{\epsilon_o} \right)^2 + R_1 \left( \frac{\epsilon}{\epsilon_o} \right)^3 \right]^2} \quad (3)$$

Beyond the peak stress point in the strain-softening region, with further straining, the compressive stress begins to decrease and the equivalent uniaxial tangent modulus becomes negative. In order to prevent the numerical difficulties associated with a negative tangent modulus, once the ultimate yield stress  $f_c$  has been reached,  $E_t$  is set to zero and the concrete behaves like perfectly plastic material (Fig. 1). This plastic response is allowed to propagate through a limited strain  $\Delta\epsilon$ , at which time the unbalanced stress is released. This process proceeds in a stepwise fashion.

### 2.2. Tensile behavior of concrete

Until the crack, initial tangent modulus  $E_c$  is used to find the maximum positive (tensile) stress. After the cracking in the concrete takes place, a smeared model is used to represent the discontinuous macro crack behavior. This cracked concrete can still carry some tensile stress perpendicular to the crack, which is termed tension stiffening. The tension stiffening factor ( $\alpha_m$  fig. 2) was assumed 0.6 in this study. In this work, a simple descending line is used to model this tension stiffening phenomenon as shown in Fig. 2. The default value of the strain  $\epsilon^*$  at which the tension stiffening stress reduced to zero is  $\epsilon^* = 0.002$ . In fig. 2,  $E_c$  and  $E_t$  are the modulus of elasticity of tensile concrete between zero to fracture strain and fracture strain to  $\epsilon^*$  respectively.  $f_t$  is the maximum stress at fracture of concrete, which has corresponding strain  $\epsilon_t$ .

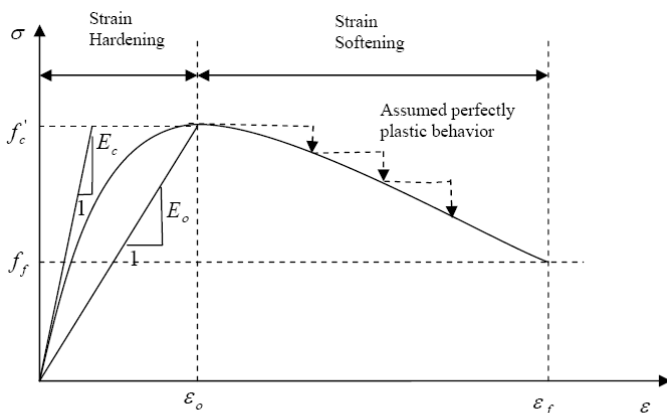


Fig. 1: Uniaxial Stress-Strain Curve for Concrete

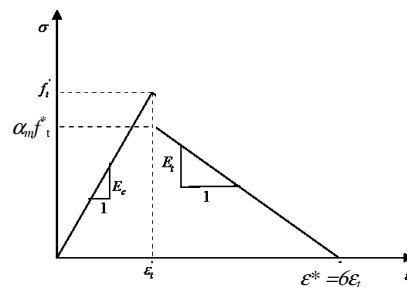


Fig. 2: Tension Stiffening Model

### 2.3 Modeling of Crack

In the concrete, when the tensile stress in the principle direction exceeds the tensile strength,  $f_t$ , of concrete, the tensile failure would occur (Desai et al. 2002). After the crack forms, both normal and shear stiffness are reduced.

## 2.4 Steel reinforcing bars

The stress-strain curve of the reinforcing bar is assumed to be elastic up to the steel yield stress ( $f_y$ ) followed by linear hardening up to the steel ultimate strength ( $f_u$ ) as shown in Fig. 3. The dowel action of the reinforcing steel is neglected and the bond between steel and concrete is assumed to remain perfect.

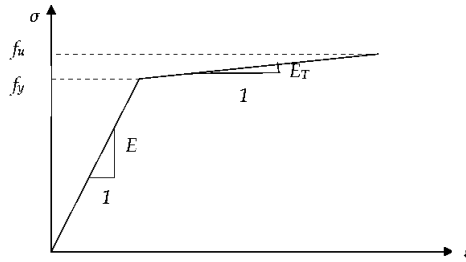


Fig. 3: Uniaxial Stress-Strain Relation for Steel

## 2.5 Mechanical Behavior of Fibrous Reinforced Concrete

The incorporation of steel fiber into concrete or mortar modifies a large number of its mechanical properties, particularly when fibers with good mechanical bond are used. As observed experimentally fibers that are randomly distributed act as micro-crack arrester, improving the ductility toughness, and reducing the crack width (Agwan 1996).

The strain at peak compressive stress  $\epsilon_{pf}$  tends to increase due to the presence of steel fiber (Soroushian and Lee 1989):

$$\epsilon_{pf} = 0.0021 + 0.007 \frac{V_f l_f}{d_f} \quad (4)$$

where  $V_f$ : volume fraction of steel fiber,  $l_f$ : length of fiber, and  $d_f$ : diameter of fiber.

While, the ultimate strength of fibrous concrete can be estimated as the strength of plain concrete known from empirical equation suggested by (Soroushain and Lee 1989):

$$f'_{cf} = f'_c + 3.6 \frac{V_f l_f}{d_f} \quad (5)$$

Strains at the peak stresses may be calculated as was derived by (Agwan 1996):

$$\epsilon_{cu} = 3011 + 2295 V_f \quad (ms) \quad (6)$$

For fibrous concrete, the modulus of elasticity can be calculated from (Mohammed 2003):

$$E_{cf} = E_c (1 - V_f) + \eta_o \eta_l E_f V_f \quad (7)$$

Where  $E_c$  and  $E_f$ : are the elastic modulus of plain concrete and fibers,

$\eta_o$ : is the orientation factor and could be taken for 0.41.

$\eta_l$ : is the length factor and was found to change widely according to the fiber length, diameter of fiber, and volume fraction.

A constant value of the product of  $\eta_o \eta_l$  which is 0.41 was proposed by Palton and Whittaker based on experimental tests carried out to study the stiffness of fibrous concrete (Mohammed 2003).

The tensile strength  $f_{tf}$  (in MPa) and its corresponding strain  $\epsilon_{tf}$  may be calculated from Soroushain and Lee (1989):

$$\hat{f}_{tf} = f_t (1 + 0.016 N_f^{1/3} + 0.05 \pi d_f l_f N_f) \tag{8}$$

$$\epsilon_{tf} = \epsilon_t (1 + 0.35 d_f l_f N_f) \tag{9}$$

Where  $f_t$ : tensile strength of concrete in MPa, and  $N_f$ : number of fibers per unit cross section area and can be calculated from Soroushain and Lee (1989):

$$N_f = \eta_o (4V_f / \pi d_f^2) \tag{10}$$

### 3. SPECIMEN DETAILS

The analyzed beams were carried out on ten beams, simply supported under single point loading. All the beams had constant span and width of 600 mm and 75 mm, respectively. Each of the three series comprised four beams of different overall depths, 400 mm, 300 mm, 200 mm and 150 mm, such that, span to depth ratios of these beams were 1.5, 2.0, 3.0 and 4.0, respectively. The first PC series of beams (plain concrete) and second FC series of beams (fiber reinforced concrete with 1.0% steel fiber by volume, aspect ratio 100 and  $d_f$  0.45mm) were without tension and web reinforcement. The third FS series of beams (fiber reinforced concrete with 1.0% steel fiber by volume, aspect ratio 100 and  $d_f$  0.45mm) had a 2-16 mm diameter mild steel bar as the main longitudinal reinforcement and 6 mm diameter mild steel bars as horizontal web reinforcement, placed at 100 mm c/c. The beam notation FS1.5 denotes the beams of FS series having span to depth ratio of 1.5, (i.e., overall depth = 400 mm). They were tested by Shah (2004). The cube strength and average cylinder splitting strength for tested beams are listed in table 1.

**Table 1: Results of control specimens**

Beam series	Average cube strength N/mm <sup>2</sup>	Average cylinder splitting strength N/mm <sup>2</sup>
PC	17.60	2.20
FC	19.00	2.80
FS	19.33	3.00

### 4. ANSYS FINITE ELEMENT MODEL

The FEA calibration study included modeling a concrete beam with the dimensions and properties as mentioned up. Due to the symmetry in cross-section of the concrete beam and loading, symmetry was utilized in the FEA; only one quarter of the beam was modeled.

### 4.1 Element Types

A solid element, **SOLID65** (fig. 4) is used to model the concrete in ANSYS. The solid element has eight nodes with three degrees of freedom at each node, translations in the nodal x, y, and z directions. The element is capable of plastic deformation, and cracking in three orthogonal directions. A **LINK8** (fig. 5) element is used to model the steel reinforcement. Two nodes are required for this element. At each node, degrees of freedom are identical to those for the SOLID65. The element is also capable of plastic deformation. A solid element, **SOLID45** (fig. 6) is used to model the loading and support plates. The solid element has also eight nodes with three degrees of freedom at each node, translations in the nodal x, y, and z directions.

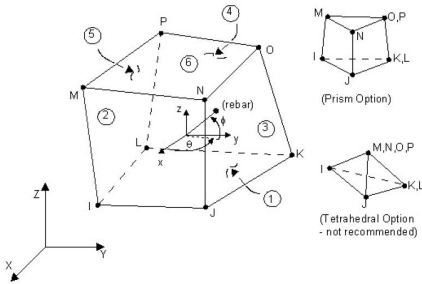


Fig. 4: Solid65 Element (SAS 2005)

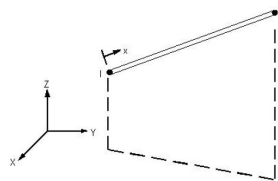


Fig. 5: Solid8 Element (SAS 2005)

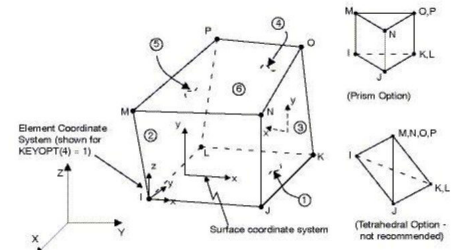


Fig. 6: Solid45 Element (SAS 2005)

### 4.2 Real Constants

The real constants for this model are shown in Table 2. Note that individual elements contain different real constants. No real constant set exists for the Solid45 element.

Table 2: Real Constant Typical Model

Real constant set	Element type	Constant			
			constant for Rebar1	Real constant for Rebar2	Real constant for Rebar3
1 (concrete)	Solid 65	Material number	4*	4*	4
		Volume Ratio	0.0033333*	0.0033333*	0.0033333*
		Orientation Angle	0°	90°	0°
		Orientation Angle	0°	0°	90°
2 (main reinforcement)	Link8	Cross-sectional area(mm <sup>2</sup> )	7.1		
		Initial strain(mm/mm)	0		
3 (secondary reinforcement)	Link8	Cross-sectional area(mm <sup>2</sup> )	28		
		Initial strain(mm/mm)	0		

Real Constant Set 1 is used for the Solid65 element. It requires real constants for rebar assuming a smeared model. Values can be entered for Material Number, Volume Ratio, and Orientation Angles. The material number refers to the type of material for the reinforcement. The

volume ratio refers to the ratio of steel to concrete in the element. The orientation angles refer to the orientation of the reinforcement in the smeared model. ANSYS (SAS 2005) allows the user to enter three rebar materials in the concrete. Each material corresponds to x, y, and z directions in the element (Fig. 4). The reinforcement has uniaxial stiffness and the directional orientation is defined by the user. In the present study the beam is modeled using discrete reinforcement. Therefore, a value of zero was entered for all real constants which turned the smeared reinforcement capability of the Solid65 element off, except in case of representation of steel fiber as a smeared layer. In this work Material Number, was entered 4 (which refers steel fiber material number), and Volume Ratio as it is assumed (its value and orientation).

Real Constant Sets 2 and 3 are defined for the Link8 element. Values for cross-sectional area and initial strain were entered. Cross-sectional areas in sets 2 and 3 refer to the reinforcement main and secondary reinforcement respectively. A value of zero was entered for the initial strain because there is no initial stress in the reinforcement.

### **4.3 Material Properties**

Parameters needed to define the material models can be found in Table 3. As seen in Table 3, there are multiple parts of the material model for each element. Material Model Number 1 refers to the Solid65 element. The Solid65 element requires linear isotropic and multilinear isotropic material properties to properly model concrete. The multilinear isotropic material uses the von Mises failure criterion along with the Willam and Warnke (1974) model to define the failure of the concrete. EX is the modulus of elasticity of the concrete ( $E_c$ ), and PRXY is the Poisson's ratio ( $\nu$ ). The modulus was based on the equation (ACI 318 2005):

$$E_c = 4750\sqrt{f'_c} \quad (13)$$

The compressive uniaxial stress-strain relationship for the concrete model was obtained using the equations in section 2 to compute the multilinear isotropic stress-strain curve for the concrete.

Typical shear transfer coefficients range from 0.0 to 1.0, with 0.0 representing a smooth crack (complete loss of shear transfer) and 1.0 representing a rough crack (no loss of shear transfer). The shear transfer coefficients for open and closed cracks were determined using the work of Kachlakev, et al. (2001) as a basis (Anthony 2004). No deviation of the response occurs with the change of the coefficient. The coefficient for the open and closed a crack were set to 0.05, 0.45 respectively (Table 2).

The uniaxial crushing stress in this model was based on the uniaxial unconfined compressive strength ( $f'_c$ ). It was entered as -1 to turn off the crushing capability of the concrete element as

suggested by past researchers (Kachlakev, et al. 2001). Convergence problems have been repeated when the crushing capability was turned on.

Material Model Number 2 refers to the Solid45 element. The Solid45 element is being used for the steel plates at loading points and supports on the beam. Therefore, this element is modeled as a linear isotropic element with a modulus of elasticity for the steel ( $E_s=20000$  MPa), and Poisson's ratio (0.3). Material Model Number 3 refers to the Link8 element. The Link8 element is being used for all the steel reinforcement in the beam and it is assumed to be bilinear isotropic. Bilinear isotropic material is also based on the von Mises failure criteria. The bilinear model requires the yield stress ( $f_y$ ), as well as the hardening modulus of the steel to be defined. The yield stress was defined as 400 MPa, and the hardening modulus was 800 MPa.

**Table 3: Material Models for Typical Model**

Material Model Number	Element Type	Material Properties						
		Linear Isotropic		Multilinear Isotropic		Concrete		
1	Solid65	EX	18248 <sup>*</sup> MPa		strain	stress	ShrCf-Op	0.05
		PRXY	0.2	Point1	0.00027806 <sup>*</sup>	5.124 <sup>*</sup>	ShrCf-CI	0.45
				Point2	0.0005	8.804 <sup>*</sup>	UnTensSt	2.8 <sup>*</sup>
				Point3	0.00075	11.875 <sup>*</sup>	UnCompSt	-1
				Point4	0.001	13.866 <sup>*</sup>	BiCompSt	0
				Point5	0.00125	14.949 <sup>*</sup>	HydroPrs	0
				Point6	0.0035	15.373 <sup>*</sup>	BiCompSt	0
							UnTensSt	0
					TenCrFac	0.6 (effective if $k_7=1$ )		
2	Solid45	Linear Isotropic						
		EX	200000 Pa					
		PRXY	0.3					
3	Link8	Linear Isotropic		Bilinear Isotropic				
		EX	200000 MPa	Yield Stss	400 MPa			
		PRXY	0.3	Tang Mod	800 MPa			
4 <sup>*</sup>	Smear d Layer (steel fiber)	Linear Isotropic		Bilinear Isotropic				
		EX	200000 MPa	Yield Stss	660 MPa			
		PRXY	0.3	Tang Mod	1050 MPa			

### 4.4 Modeling Methodology

By taking advantage of the symmetry of the beams, a quarter of the full beam is used for modeling with proper boundary conditions. This approach reduces computational time and computer disk space requirements significantly. Ideally, the bond strength between the concrete and steel reinforcement should be considered. However, in this study, perfect bond between materials is assumed.

The beam, plates, and supports were modeled as volumes. The combined volumes of the plate, support, and beam are shown in Fig. 7. The FE mesh for the beam model is shown in Fig. 8.

Link8 elements were used to create the main and secondary reinforcement.

### 4.5 Meshing

To obtain good results from the Solid65 element, the use of a rectangular mesh is recommended. Therefore, the mesh was set up such that square or rectangular elements were created (Fig. 8). The volume sweep command was used to mesh the steel plate and support. This properly sets the width and length of elements in the plates to be consistent with the elements and nodes in the concrete portions of the model. The overall mesh of the concrete, plate, and support volumes is shown in Fig. 8. The necessary element divisions are noted. The meshing of the reinforcement is a special case compared to the volumes. No mesh of the reinforcement is needed because individual elements were created in the modeling through the nodes created by the mesh of the concrete volume. However, the necessary mesh attributes need to be set before each section of the reinforcement is created.

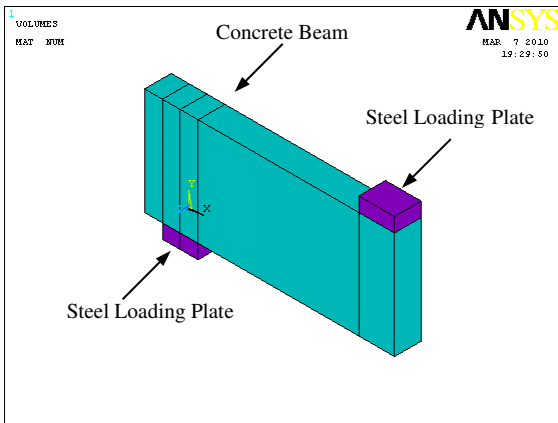


Fig.7: Volumes Created in ANSYS

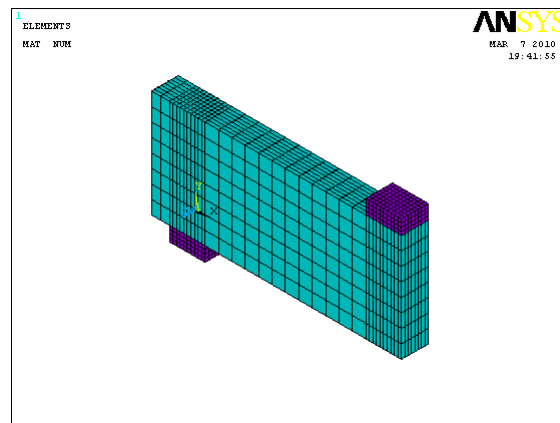


Fig. 8: Mesh of the Concrete, Steel Plate, and Steel Support

### 4.6 Loads and Boundary Conditions

Displacement boundary conditions are needed to constrain the model to get a unique solution. To ensure that the model acts the same way as the experimental beam boundary conditions need to be applied at points of symmetry, and where the supports and loadings exist. The boundary conditions for both planes of symmetry are shown in Fig. 9.

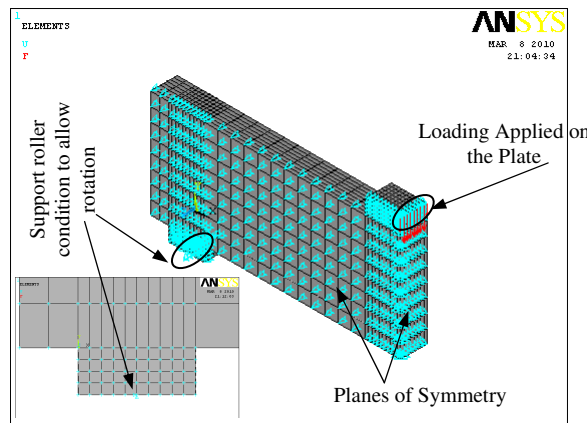


Fig. 9: Boundary Conditions of Typical Beam

The support was modeled in such a way that a roller was created. A single line of nodes on the plate were given constraint in the UY, and UZ directions, applied as constant values of 0. By doing this, the beam will be allowed to rotate at the support.

The force, P, applied at the steel plate is applied across the entire centerline of the plate.

#### 4.7 Analysis Type

The finite element model for this analysis is a simple beam under transverse loading. For the purposes of this model, the Static analysis type is utilized. The Restart command is utilized to restart an analysis after the initial run or load step has been completed. The use of the restart option will be detailed in the analysis portion of the discussion. The Sol'n Controls command dictates the use of a linear or non-linear solution for the finite element model. Typical commands utilized in a nonlinear static analysis are shown in Table 4.

**Table 4:** Commands Used to Control Nonlinear Analysis.

Analysis Options	Small Displacement
Calculate Prestress Effects	No
Time at End of Loadstep	80*
Automatic Time Stepping	On
Number of Substeps	3*
Max no. of Substeps	64*
Min no. of Substeps	1
Write Items to Results File	All Solution Items
Frequency	Write Every Substep

In the particular case considered in this work the analysis is small displacement and static. The time at the end of the load step refers to the ending load per load step. The sub steps are set to indicate load increments used for this analysis. The commands used to control the solver and out put are shown in Table 5.

**Table 5:** Commands Used to Control Output

Equation Solvers	Sparse Direct
Number of Restart Files	1
Frequency	Write Every Substep

All these values are set to ANSYS (SAS 2005) defaults. The commands used for the nonlinear algorithm and convergence criteria are shown in Table 6. All values for the nonlinear algorithm are set to defaults.

**Table 6:** Nonlinear Algorithm and Convergence Criteria Parameters

Line Search	Off
DOF solution predictor	Prog Chosen
Maximum number of iteration	100
Cutback Control	Cutback according to predicted number of iter.
Equiv. Plastic Strain	0.15
Explicit Creep ratio	0.1
Implicit Creep ratio	0
Incremental displacement	10000000
Points per cycle	13
Set Convergence Criteria	
Label	U
Ref. Value	Calculated
Tolerance	0.005
Norm	infinite
Min. Ref.	not applicable

The values for the convergence criteria are set to defaults except for the tolerances. The tolerances displacement is set as 5 times the default values. Table 7 shows the commands used for the advanced nonlinear settings.

**Table 7:** Advanced Nonlinear Control Settings Used

Program behavior upon nonconvergence	Terminate but do not exit
Nodal DOF sol'n	0
Cumulative iter.	0
Elapsed time	0
CPU time	0

The program behavior upon non-convergence for this analysis was set such that the program will terminate but not exit. The rest of the commands were set to defaults.

## 5. RESULTS AND DISCUSSION

Ten concrete deep beams were analyzed by ANSYS program. The values indicated in tables 2-7 were kept constant except those assigned by \* which were changed from one case to another. Full load deflection curves were obtained by ANSYS program. Number of iterations was made by changing Number of Substeps and Max. no. of Substeps (table 4) in solution phase to obtain full load deflection curve. It was noted that solutions diverge at load less than failure load if no adequate number of substeps were chosen. These load deflection curves were shown in figures 10-12. In fig. 10 the curves refers to non-fibrous concrete deep beams (PC-series) with span-to-depth ratios (L/D) equal 4 and 1.5 respectively. While the load deflection curves of fibrous concrete deep beam (FC-series) with (L/D) equal 4, 3, 2 and 1.5 are shown in fig. 11. And fig. 12 illustrates the load deflection curves of fibrous reinforced concrete deep beam (FS-series) with (L/D) equal 4, 3, 2 and 1.5. As mentioned previously, steel fibers were represented by using two approaches. The first approach depend on enhancement the mechanical properties of concrete (as

explained in section 2.5). In the second approach steel fibers were assumed as smeared layers embedded in solid 65 elements. In this approaches, number of cases were analyzed. First, fibers were assumed as one layer oriented in x-, y-, or z-direction. And fibers also assumed as two equal layers oriented in xy, xz, or yz directions, secondly. And the last case, fibers were assumed as three equal layers oriented in three directions. The load deflection curves show that no obvious difference was obtained by assuming steel fibers in different number of layers and their orientation. This is may attributed to that the fine meshing of deep beam will allow for good distribution of smeared layers inside the structure.

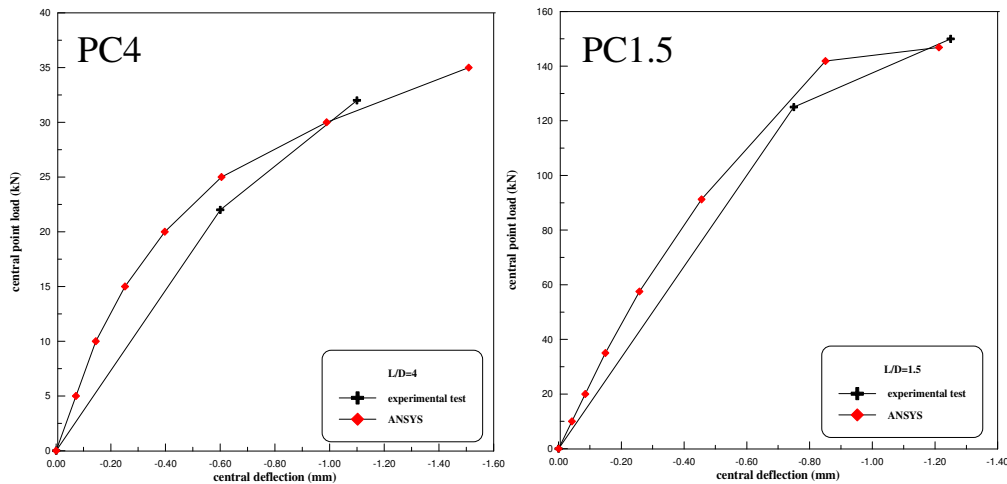


Fig. 10: Load Deflection Curves of Non-Fibrous Concrete Deep

Fig. 13 shows the crack pattern of typical deep beam (FC1.5). It can be noted that the crack pattern distributed in a larger area if the steel fiber represented as smeared layer in more than one direction. It can be also noted that three direction cracks happened in case of zero smeared steel layers which may not considered as adequate representation of two dimensional structures (deep beam). This is indicated that representation of steel fiber as smeared layers in more than one direction (two direction) more suitable for such cases.

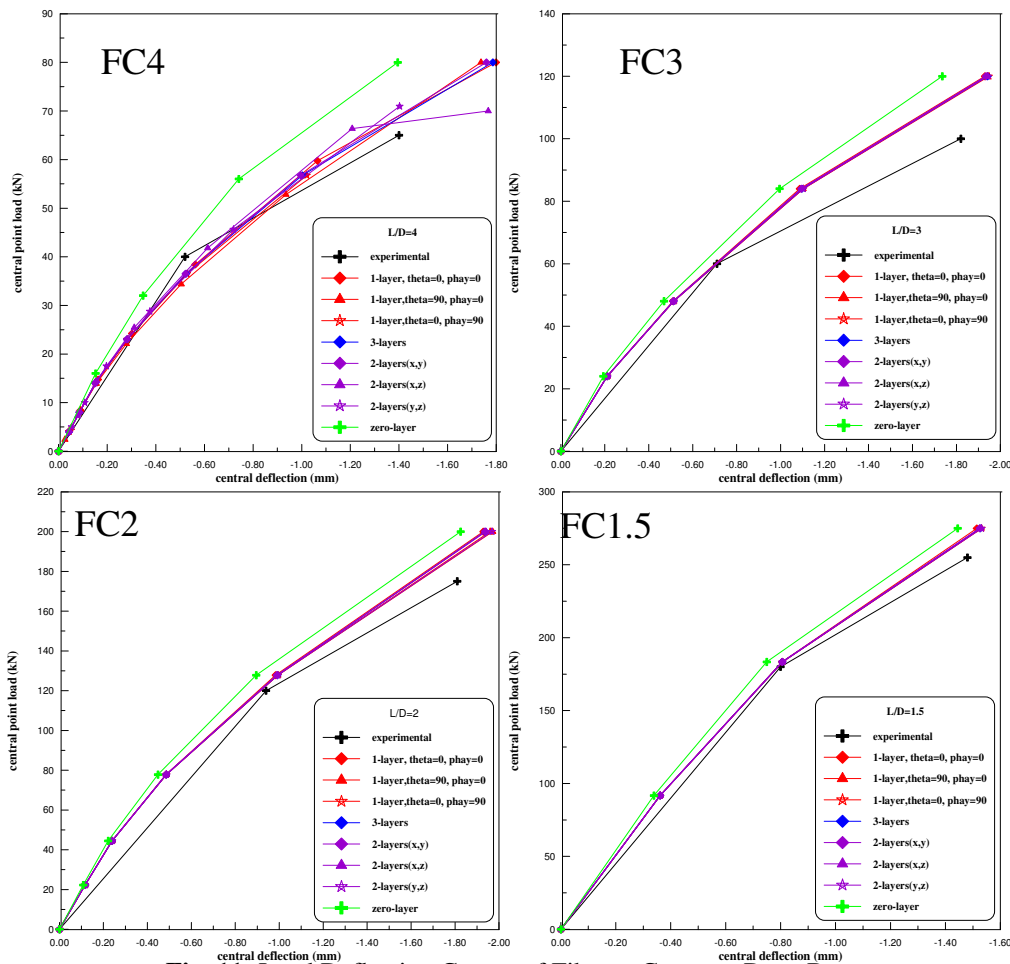


Fig. 11: Load Deflection Curves of Fibrous Concrete Deep Beam

## 6. CONCLUSIONS

Number of conclusions can be drawn by this study. Full load deflection curves can be obtained by ANSYS program in analysis of fibrous concrete deep beam if adequate representation of the structure is provided with suitable no. of substeps. Good agreement with the experimental tests was obtained in analysis of fibrous concrete deep beam by ANSYS program. Steel fibers in fibrous concrete deep beam can be represented as smeared layer in solid65 elements. Closed solutions were obtained for different number and orientations of the smeared layers of steel fibers. Representation of steel fibers in more one direction lead to distribute of crack pattern in a larger area compared to representation it in one layer. So representation of steel fibers in two equal layers in two directions may be more suitable of such cases. Solutions obtained by representation of steel fibers as smeared layers were in better agreement of enhancement mechanical properties of concrete by adding steel fibers.

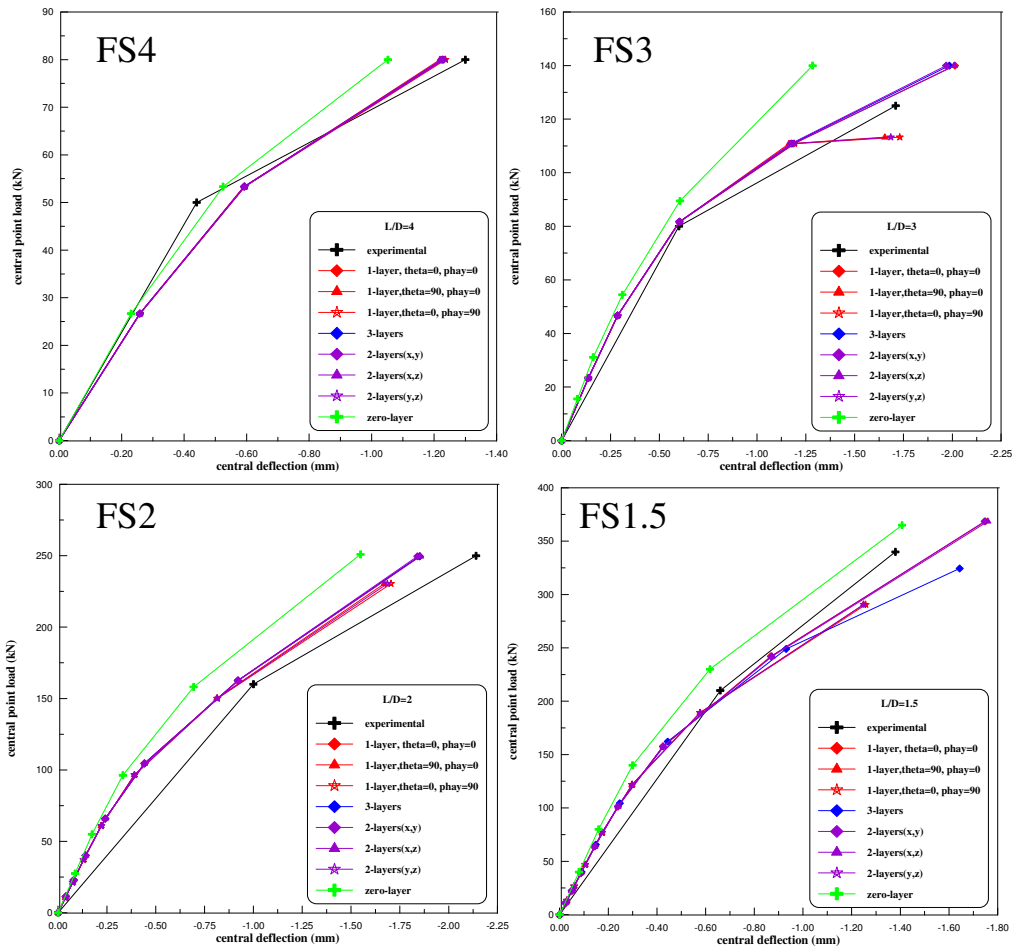


Fig. 12: Load Deflection Curves of Fibrous Reinforced Concrete Deep Beam

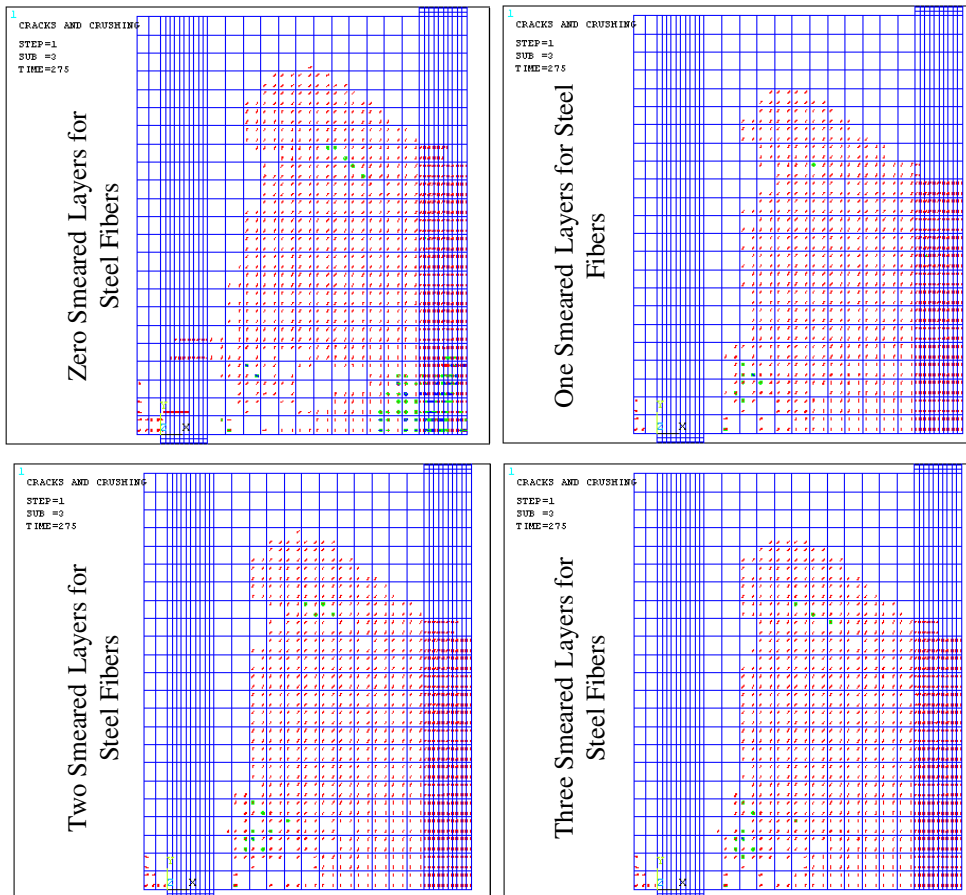


Fig. 13: Crack Pattern of Typical Beam (FC1.5)

## 7. REFERENCES

- ACI Committee 318, 2005 "***Building Code Requirements for Structural Concrete (318-05)***" and ***Commentary (318M-05)***", American Concrete Institute, Farmington Hills, MI.
- Agwan, A. A., August 1996, "***Nonlinear Finite Element Analysis of Steel Fiber Reinforced Concrete Members***", Mosul University, Iraq, pp. 237.
- Anthony J. W., 2004, "***Flexural Behavior of Reinforced and Prestressed Concrete Beams Using Finite Element Analysis***", M. Sc. Thesis, Marquette University, pp. 73.
- Desai, Y. M.; Mufti, A. A.; and Tadros, G., 2002, "***User Manual for FEM PUNCH, Version 2.0***", ISIS Canada.
- Kachlakev D. I., "***Finite Element Analysis and Model Validation of Shear Deficient Reinforced Concrete Beams Strengthened with GFRP Laminates***" California Polytechnic State University, (Cited by Anthony 2004).
- Lihua, X., Yin, C., Jie, S., and Dongtao, X., 2008, "***Nonlinear Finite Element Analysis of Steel Fiber Reinforced Concrete Deep Beams***" Wuhan University, Journal of Natural Science, Vol.13 No.2, 201-206
- Madana, S.K., Kumar, G. R. and Singh, S.P., 2007 "***Steel Fibers as Replacement of Web Reinforcement for RCC Deep Beams In Shear***" Asian Journal of Civil Engineering (Building And Housing) Vol. 8, No. 5, Pages 479-489
- Mohammed, A. A., 2003, "***Flexural Behavior of Rectangular Fibrous Concrete Slabs Allowing for Membrane Action***", Ph. D. Thesis, University of Technology, Baghdad, pp.190.
- Remigijus S. and Gediminas M., 2007, "***The Influence of Shear Span Ratio on Load Capacity of Fiber Reinforced Concrete Elements with Various Steel Fiber Volumes***" Journal of Civil Engineering and Management, Vol. XIII, No 3, 209–215.
- Saenz, and Luis, P., 1964, "***Discussion of Equation for the stress-strain curve of concrete***' by ***Prakash Desayi and S. Krishnan***", ACI Journal, V. 61, N. 9, pp. 1229-1235.
- SAS ANSYS 10.0, ***Finite Element Analysis System***", SAS IP, Inc., U.S.A., 2005.
- Shah, R. H., May 2004, "***Crack and Deformation Characteristics of SFRC Deep Beams***" IE (I) Journal.CV, Vol 85, pp. 44-48.
- Soroushian, P. and Lee, C. D., September 1989, "***Constitutive Modeling of Steel Fiber Reinforced Concrete under Direct Tension and Compression***", Proc. Of the International Conference on Recent Developments in Fiber Reinforced Cements and Concrete, Cardiff (U.K.), Es. Swamy and Barr, Elsevier Applied Science, pp. 363-377.
- Willam, K. J.; and Warnke, E. P., 1974, "***Constitutive Model for Triaxial Behaviour of Concrete***", ***Seminar on Concrete Structures Subject to Triaxial Stresses***", International Association of Bridge and Structural Engineering Conference, Bergamo, Italy, pp. 174.